ISSN: 0067-2904

Effect of Order of Reagents Addition on Optical and Structural Properties of CdS Quantum Dot Prepared by Chemical Bath Deposition Technique

F. I. Nwabue[1*], E. C. Oroke[2], D. U. Onah[3], F.S. Nworie[1], I.I. Ikelle[1]
[1]*Department of Industrial Chemistry, Ebonyi State University, P.M.B. 053 Abakaliki- Nigeria*
[2]*Department of Science Technology, The Federal Polytechnic, P.M.B. 5351 Ado-Ekiti-Nigeria*
[3]*Department of Industrial Physics, Ebonyi State University, P.M.B. 053Abakaliki-Nigeria*

Received: 13/4/2022 Accepted: 25/3/2023 Published: 30/3/2024

Abstract

Cadmium sulfide quantum dots were synthesized and deposited on glass substrates by chemical bath deposition (CBD) technique using cadmium sulfate and thiourea solutions in the presence of a 4,4'-(1,2-ethanediyldinitrilo)bis-(2-pentanone) (EDDBP) tetradentate ligand as a complexing agent. The order of reagents addition was varied to deposit films that were characterized for their surface morphological, optical, structural, and solid-state properties using a scanning electron microscope (SEM), a UV-visible spectrophotometer, an X-ray diffractometer (XRD), and Brunauer-Emmet-Teller (BET) analyses. The optimal condition for film deposition using the normal sequence of reagents addition was found at pH 8-12 and 298-353 ± 1K and gave films of 2.40-321.06 nm thickness, while the variation in the order of reagents addition gave improvements in the film properties. The optical properties and the observed direct band gaps (1.75-3.16 eV) of the films suggest usage in electroluminescent and solar cell devices since they have a first-order transition. The XRD patterns of the quantum dots indicated hexagonal wurzite structures, while the BET confirmed their mesoporous and nanonature.

Keywords: Tetradentate-Schiffbase, CdS quantum dot, Electro-luminescent device, Solar cells, Order of reagents addition.

1. Introduction

Cadmium sulfide quantum dots (CdS QDs) have been widely studied because of their numerous applications as a window layer in quantum dot photovoltaics [1, 2]. It is also very important as a window layer in the highly efficient polycrystalline Copper Indium Gallium Sulfide (CIGS) and copper indium gallium telluride, (CIGT) [3,4], which are *n*-type semiconductors with wide direct band gap energy and exist in two crystalline phases of hexagonal wurzite and cubic zinc-blend structures with unique high electron affinity [5]. CdS QDs have been used as *n*-type materials for the formation of a heterojunction in some photovoltaic systems, such as copper indium selenide (CIS) [6], copper indium gallium diselenide (CIGD) [7], and cadmium telluride (CdTe) [8].Quantum dots (QDs) are semiconductor nanocrystals with a typical size of 2-10 nm and whose electrons are confined in three directions. They are semiconductors with electronic properties closely related to the size and shape of the individual crystals. This implies that their particle sizes are similar to those of the exciton Bohr radius or the de Broglie wavelength [8, 9]. QDs have attracted considerable attention from researchers in nanotechnology. This is obviously because of their unique properties and the possibility of their manipulation according to the required application [9]. A

*Email: ikennanwabue@gmail.com

number of chemical and physical methods have been used to deposit CdS QDs in alkaline and acidic media [4]. Some of these methods include pulsed direct current magnetron sputtering [5], metal organic vapour phase epitaxy[10], and chemical solution deposition [4,11,12]. However, each of these methods has its merits and demerits. For instance, it has been reported that obtaining stoichiometric CdS by evaporation technique is difficult, while the high temperature required in the deposition of CdS using spray pyrolysis is inconvenient [13].Chemical bath deposition (CBD), also known as the solution growth deposition technique, is the controlled growth of metal chalcogenides or oxides, usually in a basic medium, through ion-by-ion deposition on a glass substrate, resulting in the formation of quantum dots [14,15]. Although CdS polycrystalline films grown by the CBD method yield a poor crystalline quality in comparison with films deposited by other techniques, they have been proven to be the most suitable for CdTe-based solar cells, as a maximum efficiency of 16.5% has been achieved with a window layer grown by the CBD technique [14]. The simplicity of CBD, its low temperature requirement, cost effectiveness and large area deposition are the reasons why it is a preferred technique for the preparation of QDs with optimal features for device applications [16].The choice of organic complexing agents (OCA) used in QDs preparation affects the optical, solid-state and surface morphological properties of the deposited thin films [4,17]. This study focused on using a tetradentate Schiff base ligand, EDDBP, as a complexing agent in the synthesis of CdS QDs by the CBD method. The effects of the order of addition of synthesis reagents on the deposition process as well as the optical, structural, surface, and solid-state properties of the prepared quantum dots have been studied.

2. Experimental

2.1. Reagents and materials

All the reagents used for the work were of analytical grade; they were used without further purification except where otherwise stated. Deionized water was used in the preparation of solutions.

2.2. Glass substrate preparation

The choice of the substrate has an impact on the film quality and properties[18].The CdS-QDs were deposited on commercial glass slides, each with dimensions of 10.0 × 76.2 × 1.0 mm, using the CBD technique as reported elsewhere [17,18]. The glass substrates were firstly cleaned with detergent using deionized water and then dipped in hydrochloric acid (10%) for 2 hours. Finally, these substrates were dipped into acetone for an hour, after which they were rinsed with deionized water and dried in the air for an hour. The cleaning and degreasing process ensures dirt removal and the provision of nucleation centers on the surface of the glass substrate for growth, as well as high adhesion and uniformity of the deposited films. Table 1 shows the substrate classification for the ease of identification of analyses performed on them.

Table 1: Substrate classification and description based on analysis performed

S/N	Study type	Substrate code	Description
1	Optimization of pH	C1-C11	pH 2-12
2	Effect of temperature	C9	303, 323 and 353 K
3	Effect of order of addition of reagents	A, B and C sequences	(A) Chalcogen-Metal salt-Buffer-Ligand. (B) Ligand-Chalcogen-Buffer-Metal salt. (C) Metal salt-Chalcogen-Buffer-Ligand.

Where A, B and C in S/N 3 are order of reagents addition codes

2.3. Preparation of EDDBP

The complexing agent EDDBP was prepared as reported elsewhere [19]. Ethylenediamine (6.6 mL) was gently added by stirring with acetyl acetone (1:2 mole ratio) (20.5 mL) in a beaker, both liquids having previously been chilled in an ice-salt mixture for 30 minutes. As the mixture solidified, it was liquefied by very gentle heating. The reaction was observed to be exothermic, and, at first, there was the formation of a whitish solid, but as more ethylenediamine was added, it became hot and a deep golden yellow. However, stirring continued until crystallization started, leading to the formation of a cream-coloured cake. The product was recrystallized twice from carbon tetrachloride, giving a whitish crystal, with a m.p. of 381 ±1 K and a yield of 92%. Spectral analysis of the reagent was reported by UV-visible, FT-IR, and ^{1}H NMR, according to the literature [20,21].

2.4. Preparation of CdS quantum dots

CdS QDs were synthesized and deposited on a glass slide from a mixture of $CdSO_4.8H_2O$ (10 mL of 0.1 M), EDDBP (5 mL of 2.23×10^{-3} M), and thiourea solution (10 mL, 0.2 M). The mixture was adjusted to an ionic strength of 0.1 M and a pH of 8 to 12 with NH_4Cl solution (0.5 M) and drops of NH_3(28%),and HCl, respectively. The mixture was then made up to 100 mL with deionized water. The glass slide was dipped into the mixture, which was stirred at 78 rpm for 2 hours at 303, 323 or 353 ± 1 K. The slide was removed, washed using deionized water (5 mL), and dried in the air for 1 hour. The slide was kept in a desiccator for further drying and preservation for subsequent characterization.

2.5. Effect of temperature on film deposition

A similar procedure as in section 2.4 was followed, and the experiments were conducted at three temperatures: 303, 323, and 353 K ± 1 with stirring to promote ion-by-ion heterogeneous growth on the substrate.

2.6. Effect of pH on film deposition

An optimization study was conducted in the pH range 2-12, prepared with ammoniacal buffer and diluted HCl, adjusted with a pH meter, the HachSension 3 pH meter, from Hach Company, USA, and standard pH paper.

2.7. Determination of dielectric constant and refractive index of films

The refractive index (n), which has a direct relationship with the reflectance of the dots, was calculated using Equation 1 as previously reported [2], and the dielectric constant (ε) was calculated using Equation 2 [22].

$$n = \frac{(1+ R^{1/2})}{(1-R^{1/2})} \quad \text{..... (1)}$$

$$\varepsilon = n^2 \quad \text{..... (2)}$$

Where ε is the dielectric constant and R is the reflectance of the quantum dots.

2.8. Effect of order of addition of reagents on the deposited CdS-QDs

The early growth stages of semiconducting QDs have a direct bearing on their physical and chemical properties [18]. For the investigation of the effect of the order of addition of reagents on the films and their properties, the same reagents were used, but the order of their addition was varied from pH 8-10 from the conventional sequence: metal salt-ligand-thiourea-buffer to the following sequences:

Sequence A: Thiourea-metal salt-buffer-ligand.
Sequence B: Ligand-thiourea-buffer-metal salt.
Sequence C: Metal salt-thiourea-buffer-ligand.

2.9. Characterization of CdS QDs

The optical and solid-state properties of the films were characterized by UV-Visible spectroscopy using a Genesys10s UV-Visible spectrophotometer, Fischer Scientific Inc., Madison, WI, USA. The absorbance and transmittance values of the films were obtained in the range of 300-1100 nm at 303 K ± 1. SEM analysis of the films was done using a computer-controlled digital scanning electron microscope, PhenomProx, Phenom World, at Eindhoven, Netherlands, with an acceleration of 15 kV and a magnification of X 290-400. XRD patterns of the films were measured on a brukerD8 discover diffractometer, equipped with a Lynx Eye detector, under Cu-Kα radiation (l = 1.5405 Å). Data were collected over the 2θ = 10-90^o range, scanning at 0.010^{o}min^{-1} and 192 s per step. The samples were placed on a zero-background silicon wafer slide. The pore textural properties of the quantum dots, including the specific BET pore surface area and pore size distributions, the nitrogen adsorption and desorption isotherms, were measured on an ASAP 2020 adsorption apparatus (micro meritics). Samples were first dried under vacuum (10^{-4} bar) at 400 K for 20 hours and then degassed again under vacuum (10^{-9} bar) at 393 K for 16 hours. The samples were backfilled with nitrogen, transferred to the analysis system, and then again degassed under ultrahigh vacuum at 373 K overnight. The BET-specific surface area was calculated using the non-local density functional theory (NLDFT) model, while the pore size was derived from the sorption curves of the films. The optical band gaps of the CdS thin films were estimated using the optical absorption theory expressed in Equation 3.

$$\alpha h\upsilon = A[h\upsilon - E_g]^n \quad \ldots\ldots\ldots\ldots\ldots\ldots (3)$$

Where hυ is the incident photon energy, E_g is the energy band gap, *n* is ½ for allowed direct transitions and 2 for allowed indirect transitions, α is the absorption coefficient of the QDs, and A is a constant of different transitions [23]. The extrapolation of the straight line curve of plots of $[\alpha h\upsilon]^2$ against photon energy (hυ)at the intercept gives the optical band gap of the CdS QDs. The thickness of the as-deposited quantum dots was obtained using the gravimetric method [24]. The weight of the glass slides was taken before and after the deposition of the films using a high-sensitivity digital electronic micro-analytical balance (accuracy and precision: 10^{-5} g), Mettler-Toledo International Inc., Columbus, Ohio, USA, and taking the film density as the bulk density.

3. Results and discussion

3.1. Effect of temperature on the deposited quantum dots

Table 2 shows the effect of bath temperature on the thickness, refractive index, dielectric constant, band gap, and nature of the films deposited at pH 10. Figure 1 shows the graph of $(\alpha h\upsilon)^2$ versus photon energy (hυ) while Figure 1 shows the graph of percentage transmittance against wavelength.

Table 2: Effect of bath temperature on thickness, refractive index, dielectric constant, band gap and nature of films deposited at pH10

Film	T(K)	t (nm)	n	ε	E_g (eV)	Nature of the as- deposited film
C9	303	7.43	1.23	1.53	2.95	Greenish yellow, adherent, homogeneous and very thin
C9	323	10.25	1.31	1.63	2.58	Thin film, light yellow, adherent, homogeneous and transparent
C9	353	26.04	1.26	1.62	2.75	Film is yellowish, adherent, transparent and non-homogeneous

Where T = temperature, n = refractive index, ε = dielectric constant, t = film thickness and E_g = band gap.

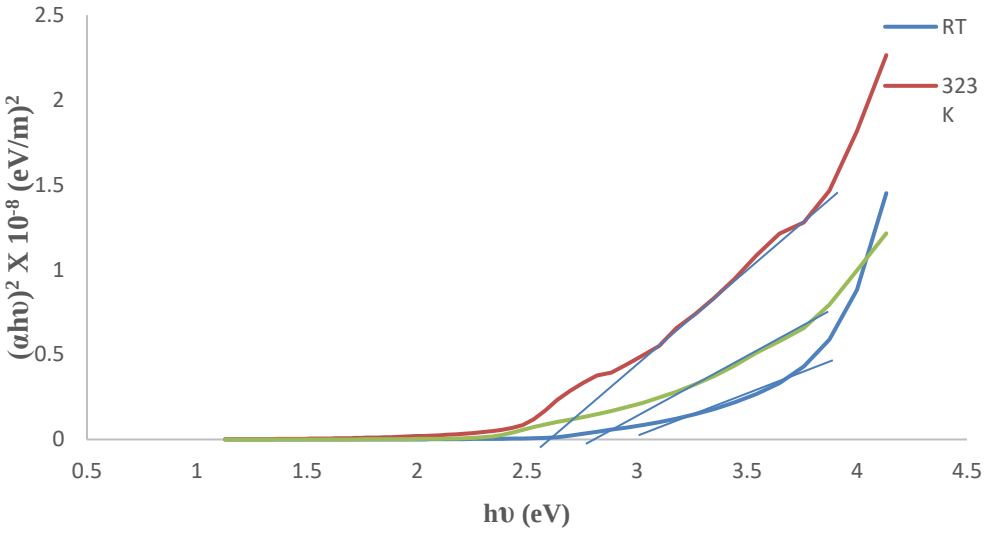

Figure 1: Graph of $(\alpha h\upsilon)^2$ against photon energy ($h\upsilon$) for the as-deposited CdS QDs in ammoniacal buffer,pH10, at various temperatures; where RT = 303 K.

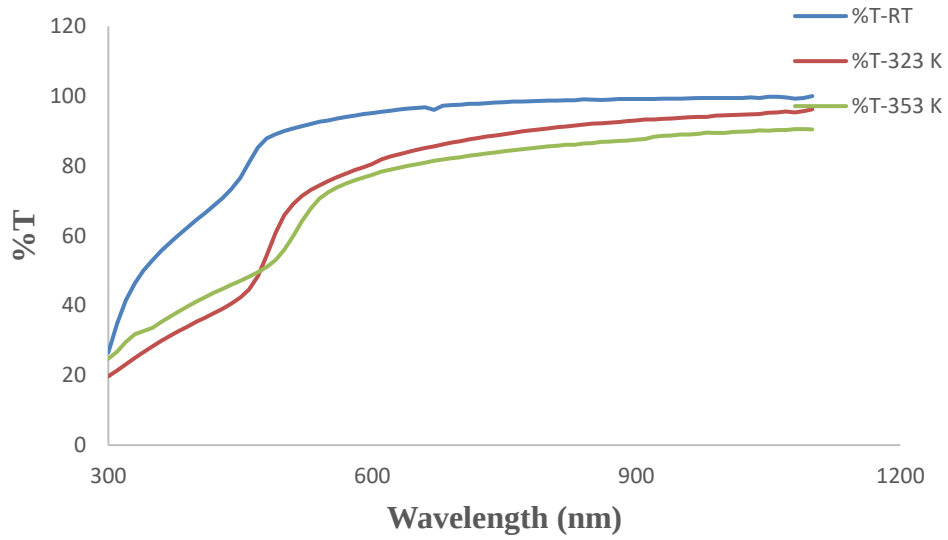

Figure 2 : Graph of the percentage transmittance of the as-grown CdS-QDs in ammoniacal buffer, pH10, at various temperatures, where RT = 303 K.

Figure 2 shows a direct dependence of the percentage transmittance of the deposited films on the chemical bath temperature, and this could be due to an improvement in the crystalline microstructure of the films with fewer scattering defects. The high T% values of 75-95% indicated a potential use of the quantum dots as a photoluminescent device and in an *n*-type window layer for a thin heterojunction solar cell.

3.2. Effect of pH on the thickness of film

The thickness of the films was calculated using the following Equation (4)

$$t = \frac{M}{2\rho A} \quad \text{..... (4)}$$

Where t is the film thickness, M is the mass of the quantum dots, ρ is the density of the CdS, which is 4.82 g/cm^3, and A is the area covered by the quantum dots [4].The effect of pH on the as-deposited CdS-QDs thickness is summarized in Table 3.

Table 3: Effect of pH on the thickness and nature of the as-deposited CdS film

Film	pH	Thickness (nm)	Nature of Film
C1	2	2.40	Colourless but adherent
C2	3	2.10	Colourless, non-homogenous but adherent
C3	4	1.80	Colourless, non-homogenous
C4	5	3.30	Colourless, sparsely scattered on the substrate (non-uniform), non-transparent but adherent.
C5	6	16.70	Pale yellow, uniformly deposited, thin, non-homogeneous but adherent.
C6	7	18.40	Light yellowish, adherent, transparent, thin and smooth but non-homogeneous
C7	8	321.06	Very yellowish, dense, uniform, adherent, smooth and homogeneous film
C8	9	287.92	Adherent, yellowish, transparent, faint, non-uniform, poor surface area coverage but smooth film.
C9	10	26.04	Thin, yellowish, adherent and transparent
C10	11	152.40	Adherent, homogeneous, smooth but thicker than at pH 10
C11	12	77.00	Adherent, thin, homogeneous and transparent.

Table 3 shows that the deposition of the films in an acid medium gave rise to generally non-homogeneous films of low thickness, while in an alkaline medium the deposited CdS-QDs were homogeneous with appreciably high film thickness except at pH 10.These results indicate the importance of a complexing agent in the deposition process of QDs. The suggested reaction steps for the deposition of the CdS-QDs using a tetradentate ligand at pH 8-10 are given in Equations 5- 12:

$$CdSO_4 + 4H_2O \rightleftharpoons [Cd(H_2O)_4]^{2+} + SO_4^{2-} \quad \text{..... (5)}$$

$$H_2EDDBP \rightleftharpoons HEDDBP^- + H^+ \ (pKa = 8.25) \quad \text{..... (6)}$$

$$HEDDBP^- \rightleftharpoons EDDBP^{2-} + H^+ \ (pKa = 10.5) \quad \text{..... (7)}$$

$$(NH_2)_2C{=}S + OH^- \rightleftharpoons (NH_2)_2C{=}O + SH^- \quad \text{..... (8)}$$

$$[Cd(H_2O)_4]^{2+} + HEDDBP^- \rightleftharpoons [CdHEDDBP]^+ + 4H_2O \ (pH\ 8\text{-}9) \quad \text{..... (9)}$$

$$[CdHEDDBP]^+ + SH^- \rightleftharpoons CdS + H_2EDDBP \ (pH\ 8\text{ - }9) \quad \text{..... (10)}$$

$$[Cd(H_2O)_4]^{2+} + EDDBP^{2-} \rightleftharpoons CdEDDBP + 4H_2O \ (pH\ 10) \quad \text{..... (11)}$$

$$CdEDDBP + SH^- \rightleftharpoons CdS + HEDDBP^- \ (pH\ 10) \quad \text{..... (12)}$$

At low pH, the undissociated H_2EDDBP and its protonated forms (H_3EDDBP^+andH_4EDDBP^{+2}) predominate [25], and the hydrolysis of thiourea to form the bisulfide ion SH^- (Equation 8) is limited. These conditions could be responsible for the observed formation of non-homogeneous films of low thickness at low pH. At pH 8-9, the monodissociated form of the ligand, $HEDDBP^-$,predominates, leading to the possible formation of a relatively unstable cationic complex, $[CdHEDDBP]^+$, which readily reacted with SH-to form CdS as shown in Equations 9 and 10. This is probably the reason for the observed increase in film thickness (287.92-321.06 nm) and homogeneity [26]. At pH 10,the completely dissociated ligand $EDDBP^{-2}$predominates, and this may have resulted in the formation of a more stable neutral complex, CdEDDBP, which probably underwent a slow thiolysis with SH to form CdS (Equations 11 and 12). This is the most likely reason for the observed decrease in the film thickness (26.04 nm). The increase and decrease in the film thickness observed at pH

11 and 12, respectively, can be explained in terms of the CdS formation from unstable and stable cadmium hydroxo-mixed-ligand complexes, respectively.

3.3. Effect of order of addition of reagents

The order in which the reagents were added to the chemical bath was in three different sequences, and the observed effects on the deposited film properties are shown in Table 4. Altering the conventional order of addition of the reagents (metal salt, ligand, thiourea, and buffer) in the bath showed a faster film deposition process and reduced film thickness, which was less homogeneous, and more uniform, but optically reflective and adherent. Physical observation of the deposition under sequence C showed that quantum dots started depositing on the substrate within 25 minutes, while for sequences A and B it took about 45 minutes. There was a change in colour of the deposited films from yellow to orange at pH 10 for sequences A, B, and C because of the addition of the reagents. The formation of orange-coloured films had been reported earlier [27] and indicated the formation of the second crystalline form of CdS besides the yellow-crystalline form, which was deposited at all other pHs studied. This is also indicative of its nanonature. Table 4 also showed a zero value for the band gap for films deposited at pH 9 using sequences B and C, indicating that the films could not balance the excess photons absorbed. This is evident in the very low absorption spectra recorded for the films deposited under these conditions. As it is known, QDs are crystals that are a few nanometers wide, so they are typically a few dozen atoms across and contain anything from perhaps a hundred to a few thousand atoms. From Table 5, it can be seen that varying the order of addition of reagents reduces the dots and increases the band gap. Because a small dot has a larger band gap, it requires more energy to excite an electron. This is because the frequency of emitted light is proportional to the energy; smaller dots with higher energy produce higher frequencies (and shorter wavelengths). Larger dots have more (and more closely) spaced energy levels, so they give out lower frequencies (and longer wavelengths) [23].

Table 4: Effects of the order of addition of reagents on the properties of the as-grown CdS quantum dots

pH	Order	Nature of Film	Colour	t (nm)	E_g (eV)	n	E	Maximum Time (min)
8	A	Adherent and transparent	Yellow	21.1	2.5	1.34	1.79	45
	B	Homogeneous and adherent	Yellow	3.1	2.7	1.37	1.88	45
	C	Fairly homogeneous	Yellow	4.1	2.9	1.27	1.61	25
9	A	Transparent and adherent	Yellow	16.0	2.9	0.74	0.55	<45
	B	Adherent and homogeneous	Yellow	35.0	0.0	1.26	1.59	45
	C	Adherent and transparent	Yellow	34.6	0.0	1.23	1.51	25
10	A	Adherent, reflecting, homogeneous, uniform	Orange	13.6	2.3	1.34	1.79	45
	B	Uniform deposition and adherent	Orange	9.7	2.5	1.79	3.20	45
	C	Uniform, non-homogeneous, adherent, reflecting	Orange	21.0	2.5	1.28	1.64	25

t = film thickness, n = refractive index of film and ε = dielectric constant of film`

Table 5: Comparison of properties of CdS quantum dots deposited by varying order of reagents addition

Order of addition	t (nm)	Abs (nm)	%T	Eg (eV)	n	E	Surface morphology
Normal	321.06	1.23	43.26	1.80	2.50	6.25	Homogeneous, smooth, small pinholes
A	21.10	0.80	77.80	2.50	1.34	1.79	Adherent and transparent
B	3.10	1.60	89.70	2.70	1.37	1.88	Homogeneous and adherent
C	4.10	0.69	89.80	2.90	1.27	1.61	Fairly homogeneous

3.4. Optical and solid state properties

The optical absorbance and transmittance spectra of as-deposited CdS-QDs samples at pH ranges 8-12 are shown in Figures 3a and 3b, respectively.

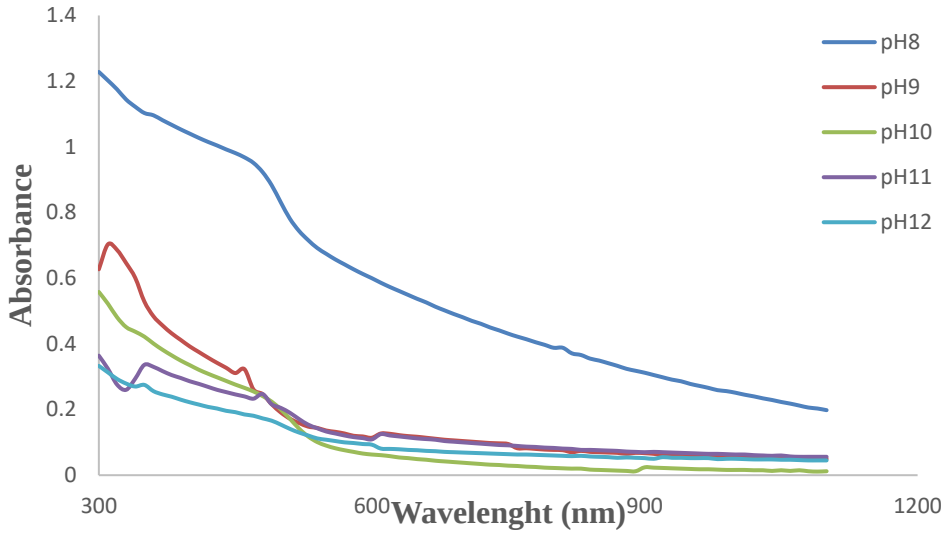

Figure 3a: Absorbance of the as-grown CdS thin films in ammoniacal buffer

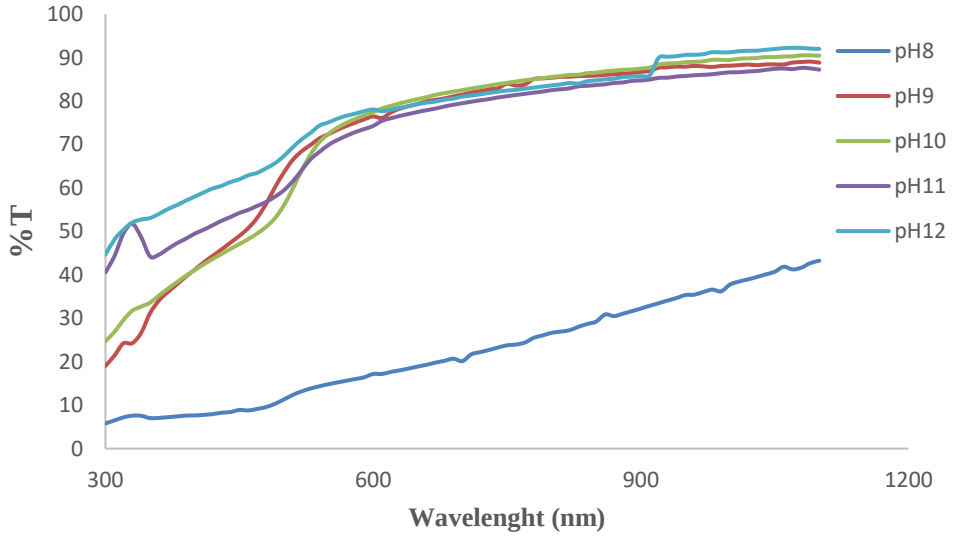

Figure 3b: T% of the as-grown CdS in ammoniacal buffer

Figure 3a shows that the CdS QDs sample grown at pH 8 has the highest absorbance value of 1.2 at 300 nm in the UV-region, which decreased exponentially through the visible to the near-infrared region. This trend suggests that the film sample is a suitable material for an anti-

reflection coating on a photovoltaic device. High absorbance in the UV region leads to reduced reflection, which enhances the short-circuit current and open-circuit voltage, thereby improving the cell efficiency [28]. CdS-QDs samples prepared at pH 9-12 showed very low absorbance in the visible and NIR regions. The low absorption of these films in these regions indicated that they could be used in the coating of windscreen and driving mirrors to prevent the dazzling effects of ultraviolet light into the eyes of the driver [29]. Figure 3b shows that the films have high transmittance values of up to 92% in the visible/NIR regions. This is an appreciable value in view of some transmittances reported [23, 24, 26-31]. The increase in the transmittance of the films deposited at high pH could be attributed to the formation of a dominant hexagonal CdS structure, and the films could serve as window materials for penetrating more light in the active regions of solar cells [30-31]. The low transmittance of these films in the UV region suggests their use as UV sensors and anti-dazzling coatings [17].

3.5. Optical constants of the deposited films

Tables 2, 4, and 5 showed that the refractive index has a direct bearing on the dielectric constants of the films. This is obvious as the dielectric constant increased with increases refractive index and vice versa. The absorption coefficient (α) of the quantum dots was obtained from the following equation:

$$\alpha = \frac{1}{t}\ln\frac{1}{T} \quad \ldots\ldots\ldots\ldots\ldots\ldots\ldots\ldots \quad (13)$$

Where t is the thickness of the film, T is the transmittance, which is equal to 10^{-A} where A is the absorbance [12,28]. In both the direct and indirect semiconductor transitions, the absorption coefficient and optical band gap (E_g) are related by Equation 3[32]. Plots of $[\alpha h\upsilon]^2$ against photon energy ($h\upsilon$) for as-deposited CdS thin films are shown in Figure 4.

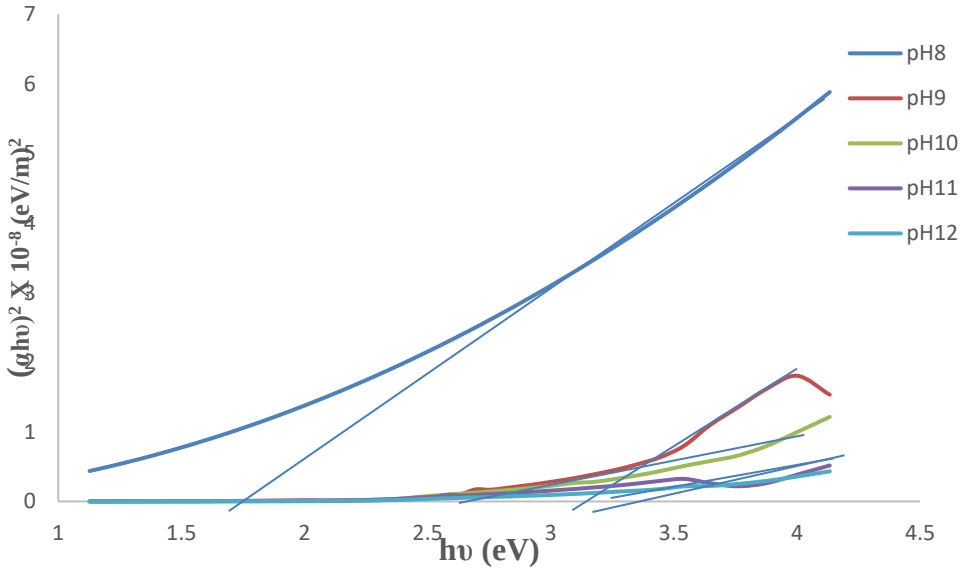

Figure 4: Graph of $(\alpha h\upsilon)^2$against photon energy ($h\upsilon$) for the as-deposited CdS quantum dots in an ammoniacal buffer

The band gaps of the film samples were determined from the extrapolations of the straight portions of Figure 4 to the energy axis. Figure 5 clearly indicates that CdS-QDs have direct transitions. The sample (C7), prepared in ammoniacal buffer at pH 8, has an energy gap of 1.75 eV. Other film samples (C8-C11), with pH ranging from pH 9-12, respectively, have energy gaps ranging from 3.17-3.54 eV. The appreciable improvement of the band gap in the present study could be linked to the new tetradentate ligand and improvement in the crystallinity of the deposited films. It is interesting to note that the band gap energy generally depends upon the

film's composition, crystal structure, particle size, and strain [33]. The wide bandgap of the CdS-QDs is important since CdS is mostly used as a window layer to maintain low series resistance [28]. Moreover, studies have shown that superior device performance is achieved when the junction is matched to the solar spectrum by increasing the band gap. These ranges of band gaps are in agreement with the values obtained in previous studies [4,34]. As a direct band gap material, the QDs could have good application in electroluminescent devices since the radiative recombination of these films is a first order transition process [28].

3.6. Surface morphology

SEM provides microscopic information on the film's surface. It is helpful in identifying the growth mode and, hence, determining the effect of the complexing agent on the as-deposited film [30]. Visually, the sample (Figure 5c) of CdS film deposited on a glass substrate at pH 10 was smooth, uniform, and reflective, with strong adherence to the substrate. This shows the formation of small holes between the particles with clearly defined grain boundaries. The observed crystallites in the films could be due to the high deposition temperature of 353 ± 1 K.

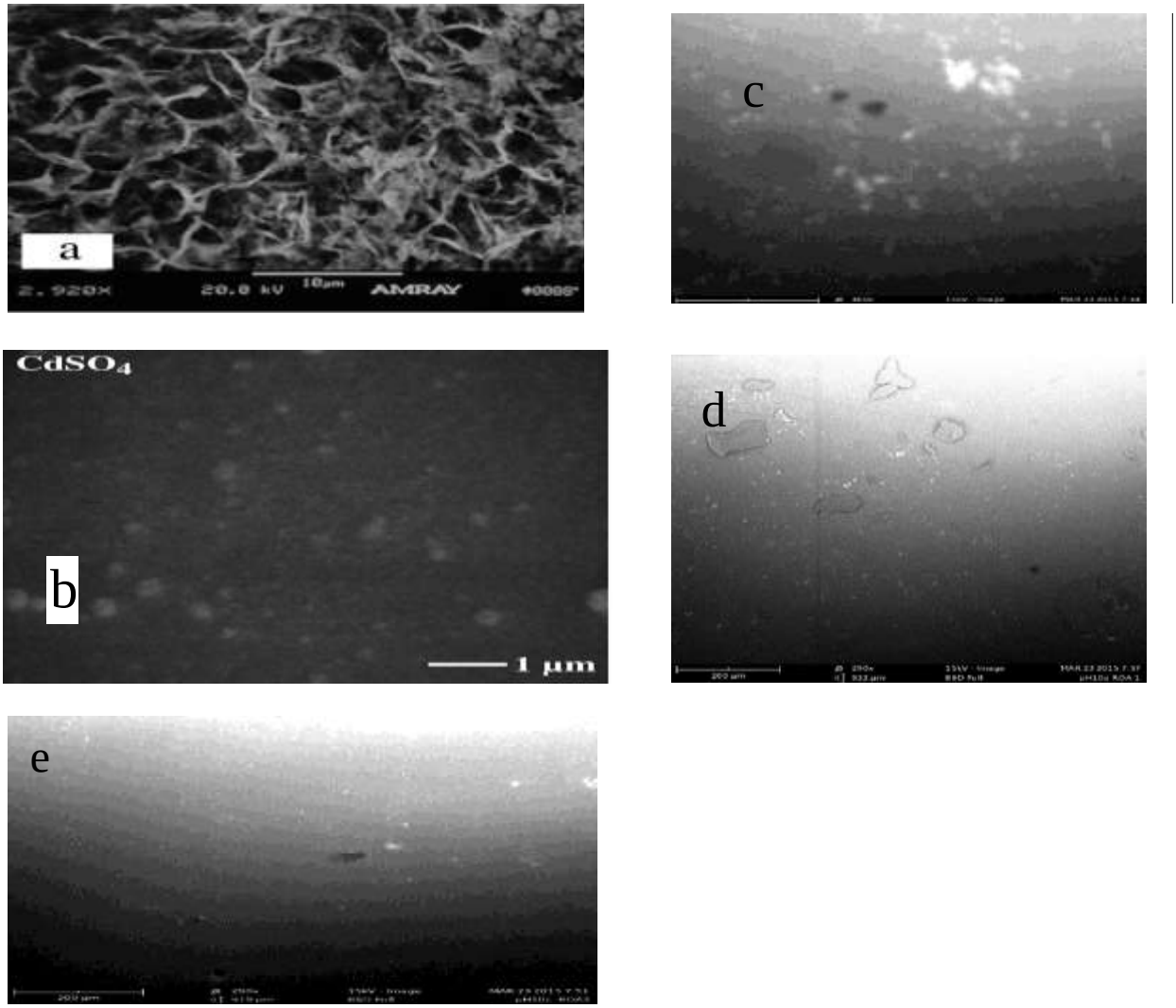

Figure 5: Comparison of the SEM (surface morphology) of CdS films deposited using NH3 at pH 11 and EDDBP at pH 10 as complexing agents

The surface roughness observed in Figures 5d and 5e could be a result of robust crystal overgrowth, which causes scattering of light and hence lowers transmission [34]. However, there appears to be a current interest in the production of rough surfaces with specific topography and chemical properties for device applications, including cellular engineering [35].Figures 5a and 5b are scans of CdS quantum dots deposited using ammonia as the complexing agent [4, 34-35] and suggest that using ammonia as the complexing agent gives porous, rough, and colloidal particles, giving rise to cluster-by-cluster deposition [31], which is undesirable. However, Figure 5b is similar to the present work, Figures 5c and 5d, with possible differences due to the source of cadmium salt used or other deposition conditions, such as the nature of the complexing agent.

3.7. Structural and solid state characterization

3.7.1 X-Ray Diffraction

The crystalline pattern of the as-deposited CdS quantum dots was examined using a powder X-ray diffraction technique (Figures 6a and 6b). This was done for samples prepared at pH 8 by the normal order of addition of reagents (Figure 7a) and sequence C with the order of addition of reagents (Figure 6b). In Figure 6a, the film showed one prominent broad diffraction peak of 2θ values approximately 18.0^o and the other two weak peaks at 2θ values approximately 52.0^o, and 62.40^o, which can be indexed as 100, 110, and 104, respectively. The excess peak broadening seen in Figure 6a could be due to the poor performance of the diffractometer used. The crystallite size (nm) was calculated from the Debye-Scherrer equation (Equation 14):

$$D = \frac{K\lambda}{\beta\cos\theta} \qquad \ldots\ldots\ldots\ldots\ldots\ldots 14$$

Where K is the Debye-Scherer constant, β is the full width at half maximum (FWHM), λ is the wavelength, and θ is the Bragg angle. The average crystal size of the particles (for Figure 6a), as calculated from the width of the XRD peaks using Equation 14, was 1.06 nm, indicating that the as-deposited CdS-QDs are nanosized. However, in Figure 6b, the diffraction peaks positioned at 2θ values approximately 26.50, 28.5, 44.50, and 63.10^o match well with the crystalline phase of CdS and can be indexed respectively to the 002, 101, 110, and 104 crystal planes as the hexagonal wurzite structure of phase β-CdS compared with data from the International Centre for Diffraction Data (ICDD) file No.10-454. Similarly, the average crystal size of the particles (for Figure 6b),as calculated from the width of the XRD peaks using equation 14, was 1.73 nm, indicating that the as-deposited CdS-QDs are nanosized. The broadness of the peaks clearly indicates that the dimensions of CdS nanoparticles are very small [36]. This has gone a long way to confirm the nanoscale nature of the as-deposited CdS-QDs (Table 5). Below 10 nm, peak broadening is so significant that the signal intensity is low, and peaks overlap and can be difficult to discern. Particles having crystalline domain sizes below 5 nm become difficult to analyze due to both broad peaks and low signal-to-noise ratios [37]. Moreover, this broadening of the peak could also arise due to the micro-straining of the crystal structure arising from defects, such as dislocation and twinning, etc. It is believed that defects of this sort are associated with the chemically synthesized nanocrystals, since they grow spontaneously during chemical reactions. As a result of this, the chemical ligand gets negligible time to diffuse to an energetically favorable site. It could also arise due to the lack of sufficient energy needed by an atom to move to a proper site for forming the crystal [38]. Above all, a report has confirmed that the diffraction peaks in nanocrystalline particles are broadened compared to single or polycrystalline solids of the same material [39].

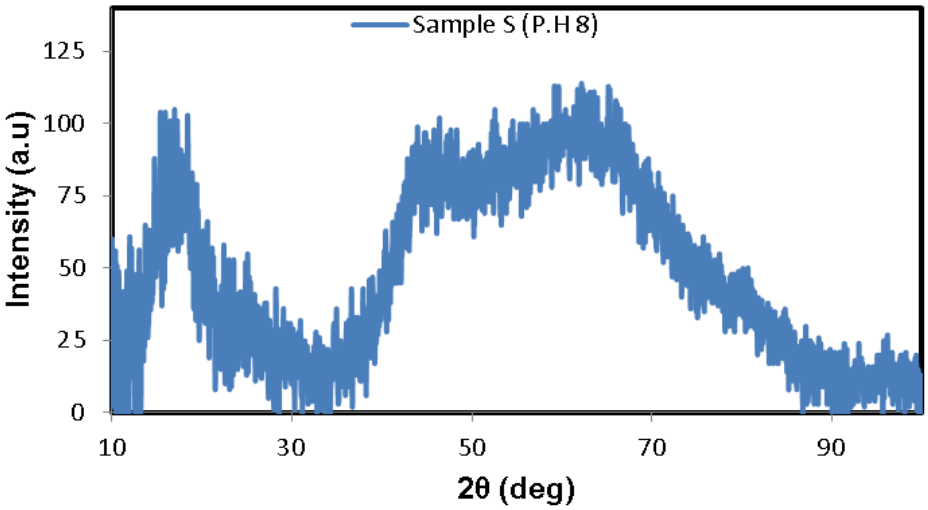

Figure 6a : XRD pattern for as-deposited CdS-QDs sample S deposited at pH 8 by the normal sequence of reagents addition

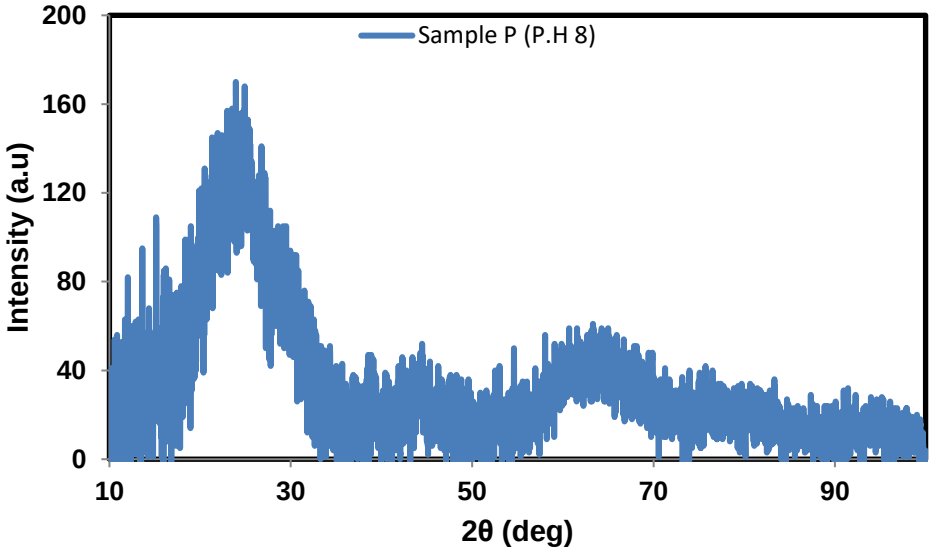

Figure 6b - XRD pattern for the as-deposited CdS-QDs sample P deposited at pH 8 by the sequence C order of reagents addition

3.7.2. BET Analysis Results

Pore size and surface area of QDs are very important properties in the study of their characteristics. Generally, as the particle size of deposited film decreases, the proportion of atoms found at the surface of the film is magnified relative to the proportion inside its volume, which results in nanoscale particle types likely to become more active and effective in a variety of applications [35,40]. Figures 7a, b, and c, and Table 5, are the results of BET analysis of the as-deposited quantum dots at pH 8 using different sequences of reagent addition. The results indicated a mesoporous surface for the deposited quantum dots. The hysteresis loops of the samples' isotherms occurred over a pressure range of 0.8-1.0 mm/Hg and shifted upward by 180, 130, and 240 cm^3/g STP for samples S, Q, and P deposited by normal sequence, sequence B, and sequence C, respectively, and these values reflect the relative pore surface areas of the QDs samples. The three samples, however, formed about the same pore size on the deposition due to their respective sequences of reagent addition.

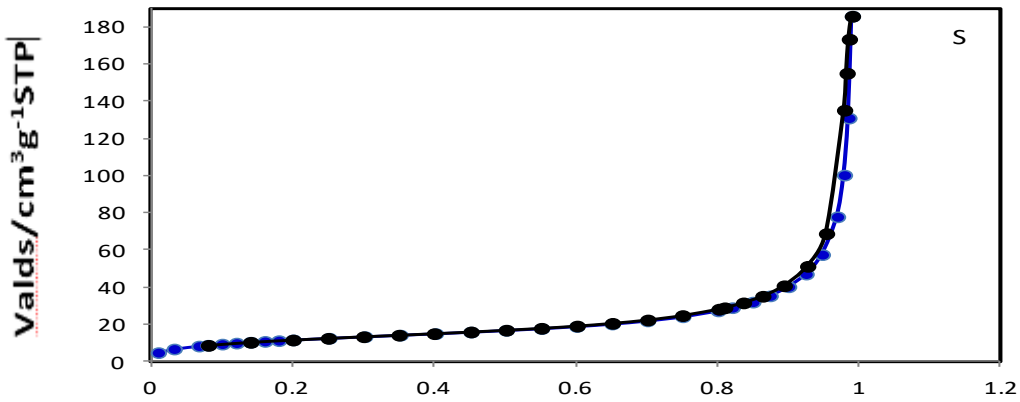

Figure 7a: BET nitrogen adsorption (black) and desorption (blue) isotherms of deposited quantum dots at pH 8 by the normal order of reagents addition

Table 6 : BET analysis of deposited thin films at pH 8 showing pore surface area and pore size

Sample	Pore surface Area (m^2/g)	Pore size (nm)
S	42.58	27.31
Q	36.19	26.26
P	57.24	26.17

***Note**: S sample was deposited by normal order of addition of reagents while Q and P samples were deposited by sequences B and C order of reagents addition*

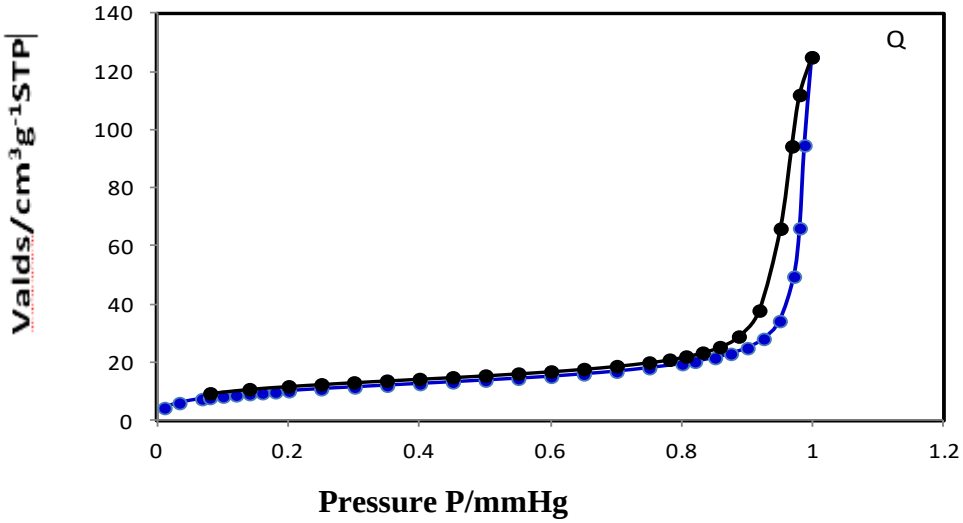

Figure 7b: BET nitrogen adsorption (black) and desorption (blue) isotherms of deposited quantum dots at pH 8 by the sequence B order of reagents addition

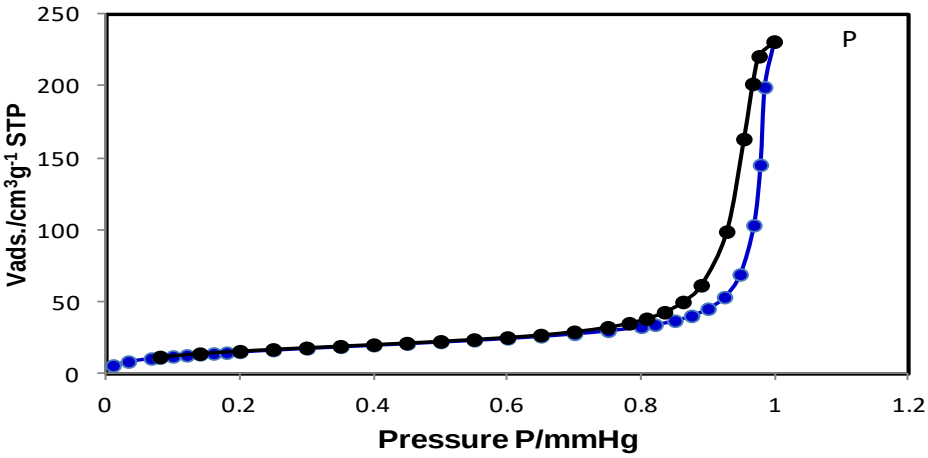

Figure 7c: BET nitrogen adsorption (black) and desorption (blue) isotherms of deposited quantum dots at pH 8 by the sequence C order of reagents addition

Table 7 : Comparison of properties of CdS films deposited using different complexing agents

S/N	Complexing Agent	pH	Abs	%T	t (nm)	Eg (eV)	Surface morphology	Reference
1	EDDBP	8-12	High in the UV regions	High in the Vis/NIR, 90-92%	26.0-321.1	1.76-3.30	Homogeneous, smooth, small pinholes	This work
2	$NaBH_4$	10	-	Low deposition, 63 %	189	2.34	Cracks formation due to high deposition	34
3	N_2H_4	10	-	High in Vis-regions	54	2.35	Homogeneous due to low deposition	34
4	NH_3	11-12	-	High in the Vis, low in the NIR.	95	2.47	Rough, crystallite overgrowth	4
5	NTA	10		High in the Vis-region	200	2.30	Rough, having small pinholes	33
6	EDTA	11	-	High in the Vis-region, 76%	-	-	Very smooth, ion-by-ion deposition	31

4. Conclusion

A chemical bath deposition technique has been used to deposit CdS-QDs on glass substrates using a tetradentate Schiff base ligand (EDDBP) as a complexing agent. The optical and solid-state properties of the CdS-QD indicate some advantages compared with other complexing agents, as summarized in Table 6.Varying the order of addition of the synthesis reagents from the conventional sequence was found to be critical for the rate and nature of deposition of the QDs (Table 3), and the method could be exploited in the preparation of QDs of varied properties for specialized applications.

Acknowledgements

The authors wish to thank the Directorate of Research, Innovation, and Commercialization, Ebonyi State University Abakaliki (EBSU-DRIC), for their financial assistance through the TET-fund research grant (Ref. No.: EBSU/TETFund/IBR/2015/10).

Conflict of interest: The authors declare that they have no conflicts of interest whatsoever.

References

[1] A. D. Compaan, A. Gupta, J. Drayton, and S. H. Lee, "14% sputtered thin-film solar cells based on CdTe", *Physica Status Solidi B.,* vol. 241, no. 3, pp. 779-782, 2004.

[2] A. O. Awodugba, O. Adetokun, and Y. K. Sanusi, "Study of optical and crystallographic properties of CBD grown CdS thin films", *International Journal of Recent Research and Applied Studies*, vol. 12, no. 3, pp. 12-23, 2012.

[3] H. Khallaf, I. O. Oladeji, G. Chai, and L. Chow, "Characterization of CdS thin films grown by chemical bath deposition using four different cadmium sources", *Thin Solid Films,* vol. 516, pp.7306-7318, 2008a.

[4] W. Vallejo, C. Diaz-Uribe, and C. Quiñones, "Optical and structural characterization of Cd-free buffer layers fabricated by chemical bath deposition. *Coatings*, vol. 11, pp. 897-912, 2021.

[5] F. Lisco, P. Kaminski, A. Abbas, K. Bass, J. Bowers, G. Claudio, M. Losundo, and M. Walls, "The structural properties of CdS deposited by chemical bath deposition and pulsed direct current magnetron sputtering", *Thin Solid Films*, vol. 582, pp. 323-327, 2015.

[6] E. B. Yousfi, T. Asikainen, V. Pietu, P. Cowache, M. Powalla, and D. Lincot, "Cadmium-free buffer layers deposited by atomic later epitaxy for Copper indium diselenide solar cells", *Thin Solid Films*, vol. 362, pp. 183-186, 2000.

[7] J. Rousset, F. Donsanti, P. Genevee, G. Renou, and D. Lincot, "High efficiency cadmium free Cu(In,Ga)Se_2 thin film solar cells terminated by an electrodeposited front contact", *Solar Energy Materials and Solar Cells*, vol. 95, vol. 6, pp. 1544-1549, 2011.

[8] E. M. Assim, "Synthesis, structure, and optical properties of nanopowders CdS: xAl (x=0, 1, 5, 10, 15 and 20%) via the sol–gel technique", *Egyptian Journal of Solids*, vol. 43, no. 1, pp. 111-125, 2021.

[9] H. N. Noori and A. F. Abdulameer, "Study of the effect of pH on the optical properties of the CdTe quantum dots", *Iraqi Journal of Science,* vol. *64, no. 2,* pp. 653-657, 2023.

[10] R. Berrigan, N. Maung, S. J. Irvine, D. Cole-Hamilton, and D. Ellis, "Thin films of CdTe/CdS grown by MOCVD for photovoltaics", *Journal of Crystal Growth,* vol. 195, no. 1-4, pp. 718-724, 1998.

[11] S. Raprasad, Y. Su, C. Chang, B. K. Paul, and D. R. Palo, "Cadmium sulfide thin film deposition: A parametric study using microreactor-assisted chemical solution deposition", *Solar Energy Materials and Solar Cells,* vol. 96, pp. 77-85, 2012.

[12] B. Schubert, B. Marsen, S. Cinque, T. Unold, R. Klenk, S. Schorr, and H. Schock, "Cu_2ZnSnS_4 thin film solar cells by fast coevaporation", *Progress in Photovoltaics: Research and Applications,* vol. 19, pp. 93-96, 2011.

[13] S. A. Zahra, "Effect of grain size on the electrical conduction mechanism for aluminum doped CdS thin films", *Journal of Electron Dev*ices, vol. 13, pp. 1494-1499, 2013.

[14] J. Aguilar-Hernandez and J. Sastre-Hernandez, "Photoluminescence studies on CdS-CBD films grown by using different S/Cd ratio", *Thin Solid Films*, vol. 511-512, pp. 143-146, 2006.

[15] N. A. Okereke and A. J. Ekpunobi, "Structural and optical studies and applications of chemically deposited lead selenide thin films", *Journal of Ovonic Research,* vol. 6, no. 6, pp. 277-283, 2010.

[16] N. K. Allouche, T. B. Nasr, C. Guasch and N. K. Turki, "Optimization of the synthesis and characterizations of chemical bath deposited Cu2S thin films", *Comptes Rendus Chimie,* vol. 13, pp. 1364-1376, 2010.

[17] A. O. Awodugba and O. Adedokun,"On the physical and optical characteristics of CdS thin films deposited by the chemical bath deposition technique", *Pacific Journal of Science and Tech*nology, vol. 12, no. 2, pp. 334-347, 2011.

[18] A. A. Oladiran, A. Oluwaseun, and S. Y. Kolawole, "Study of optical and crystallographic properties of CBD grown CdS thin films", *International Journal of Research and Reviews in Applied Sciences*, vol. 12, no. 3, pp. 420-434, 2012.

[19] F. I. Nwabue and E. N. Okafor, "Studies on the extraction and spectrophotometric determination of Ni(II), Fe(II), Fe(III) and V(IV) with bis(4-hydroxypent-2- ylidene)diaminoethane", *Talanta,* vol. 39, no. 3, pp. 273-280, 1992.

[20] M. Moreno, G. M. Alonzo-Medina, A. I. Oliva, and A. I. Oliva-Avilés, "Cadmium sulfide thin films deposited onto MWCNT/Polysulfone substrates by chemical bath deposition", *Advances in Material Science Engineering.*, vol. 2016, no. 28, pp. 10-21, 2016.

[21] L. N. H. Arakaki, J. S. Diniz, A. L. P. Silva, V. L. S. A. Filha, M. G. Fonseca, J. G. P. Espínola, and T. Arakaki, "Thermal study of chelates of Co(II), Cu(II), Ni(II), Cr(III), Mo(III), and Fe(III) with Bis(Acetylacetone)Ethylenediimine on activated silica gel surface", *Journal of Thermal Analysis Calorimetry*, vol. 97, no. 2, pp. 377-383, 2009.

[22] S. Ozkar, D. Ulku, L. T. Yıldırım, N. Biricik, and B. Gumgum, "Crystal and molecular structure of bis(Acetylacetone) ethylenediimine: Intramolecular ionic hydrogen bonding in solid state", *Journal of Molecular Structure*, vol. 688, pp. 207-221, 2004.

[23] N. Qutub and S. Sabir, "Optical, thermal and structural properties of CdS quantum dots synthesized by a simple chemical route", *International Journal of Nanoscience and Nanotechnology*, vol. 8, no. 2, pp. 111-120, 2012.

[24] D. Kathirvel, N. Suriyanarayanan, S. Prabahar, S. Srikanth, and P. Rajasekaran, "Structural, optical and electrical properties of chemical bath deposited CdS thin films", *Chalcogenide Letters*, vol. 8, no. 12, pp. 739-757, 2011.

[25] V. L. Ukoha, N. Obasi, and F. I. Nwabue, "Solvent extraction studies on Copper(II) and Silver(I) complexes of Bis(4-hydroxypent-2-ylidene) diaminoethane: separation of Ag(I) from Cu(II)", *International Journal of Chemistry*, vol. 22, no.1, pp. 15-24, 2012.

[26] V. B. Sanap and B. H. Pawar, "Growth and characterization of nanostructured CdS thin films by chemical bath deposition technique", *Chalcogenide Letters*, vol. 6, no. 8, pp. 415-419, 2009.

[27] H. I. Salim, O. I. Olusola, A. A. Ojo, K. A. Urasov, M. B. Dergacheva, and I. Dharmadasa, "Electrodeposition and characterisation of CdS thin films using thiourea precursor for application in solar cells", *Journal of Materials Science: Materials in Electronics*, vol. 27, no. 7, pp. 6786-6799, 2016.

[28] I. A. Ezenwa, "Effect of film thickness on the transmittance of chemical bath fabricated CdS thin film", *Advances in Applied Science Research*, vol. 3, no. 5, pp. 2826-2840, 2012.

[29] S. M. H. Al-Jawad, A. M. Mausa, and W. A. Taha, "Investigation of optical properties of CdS thin films by chemical bath deposition", *Um-Salama Science Journal*, vol. 6, pp.150-162, 2009.

[30] S. Dimitrijev, "Understanding Semiconductor Devices", Oxford University Press, p.182, 2000.

[31] A. Carrillo-Castillo, R. C. AmbrosioLázaro, E. M. Lira-Ojeda, C. A. Martínez Pérez, M. A. Quevedo-López, F. S. Aguirre-Tostado, "Characterization of CdS thin films deposited by chemical bath deposition using novel complexing agents", *Chalcogenide Letters*, vol. 10, no. 10, pp. 421-434, 2013.

[32] S. A. Jassim and E. M. A. Nassar,"Effect of annealing temperature on structure and optical properties of CdO nanocrystaline thin film prepare by chemical bath deposition method", *IOP Conference Series: Materials Science and Engineering*, vol. 928, ID. 072046, 2020.

[33] H. Khallaf, I. O. Oladeji, and L. Chow, "Optimization of chemical bath deposited CdS thin films using nitrilotriacetic acid as a complexing agent", *Thin Solid Films*, vol. 516, pp. 5967-5973, 2008c.

[34] K. L. Choppra, P. D. Paulson, and V. Dutta, "Thin-film solar cells: An overview", *Progress in Photovoltaics: Research and Applications*, vol. 12, pp. 92-112, 2004.

[35] Z. H. Barber, "The control of thin film deposition and recent developments in oxide film growth", *Journal of Material Chem*istry, vol.16, pp. 334-349, 2006.

[36] F. A. Hasan, M. T. Hussein, M. A. "Abdulsattar, "Structural, optical, and morphological study of the zinc oxide nano-thin films with Different thickness prepared by pulsed laser deposition technique", *Iraqi Journal of Science*, vol. 63, no. 12, pp: 5242-5254, 2022.

[37] C. F. Holder, and R. E. Schaak, "Tutorial on powder X-ray diffraction for characterizing nanoscale material". *ACS Nano*, vol. 7, pp. 7359-7365, 2019.

[38] A. Firdous, D. Singh, and M. M. Ahmad, "Electrical and optical studies of pure and Ni-doped CdS quantum dots", *Applied Nanoscience*, vol. 3, pp. 13-18, 2013.

[39] S. K. Kulkarni,"Nanotechnology: principles and practice", *Springer International Publishing, Cham, Switzerland, with Capital Publishing Company, New Delhi, India*, 3rd ed., 2015.

[40] R. Fitzpatricks, "Electromagnetic Wave Propagation in Dielectrics", http://farsiderph.utexas.Edu/teaching/jkl/lectures/node 79 htmail, 130-138. Retrieved: 01/02/2021, 2002.